DIRECT POWER CONTROL OF A DOUBLY FED INDUCTION GENERATOR BASED WIND ENERGY CONVERSION SYSTEMS INCLUDING A STORAGE UNIT

Y. DJERIRI*, A. MEROUFEL, A. MASSOUM, and Z. BOUDJEMA
Department of Electrical Engineering, University Djillali Liabes of Sidi Bel Abbes, Algeria, 22000
Intelligent Control and Electrical Power Systems –ICEPS- Laboratory
* djeriri_youcef@yahoo.fr

Abstract *: To solve intermittent availability of popular renewable energy source based on wind energy, this paper deals with the design, analysis and simulation of a wind turbine associated with a storage unit to generate a constant active power through the grid for all wind conditions. A Doubly Fed Induction Generator (DFIG) allowing a large speed variation and so a large range of wind is employed. The incorporation of a battery or other energy storage device in the DC-link enables temporary storage of energy. Traditionally, control of DFIG is achieved by Flux Oriented Control (FOC), this technique decouples the rotor currents into active and reactive components; control of the active and reactive powers is achieved indirectly by controlling the input currents by using of classical Proportional-Integral (PI) controllers. However this controller depends highly on parameter variations of the DFIG. Direct Power Control (DPC), without inner current control loops, produces a fast and robust power response. Simulation results on a 1.5 MW DFIG system are provided to demonstrate the control strategy and the large interest of energy storage in such wind energy conversion systems (WECS).*

Keywords *: Double fed induction generator, direct power control, storage unit, wind energy.*

1. Introduction

Since fifteen years, the concept of the variable speed wind turbine (VSWT) equipped with a doubly fed induction generator (DFIG) has received increasing attention due to its noticeable advantages over other wind turbine concepts [1-2]. In the DFIG concept, the stator is usually connected directly to the three-phase grid; the rotor is also connected to the grid but via a transformer and two back-to-back converters (Fig. 1). Usually, the rotor-side converter controls the active and reactive power and the grid side converter controls the DC-link voltage and ensures operation of the converter at a unity power factor [1].

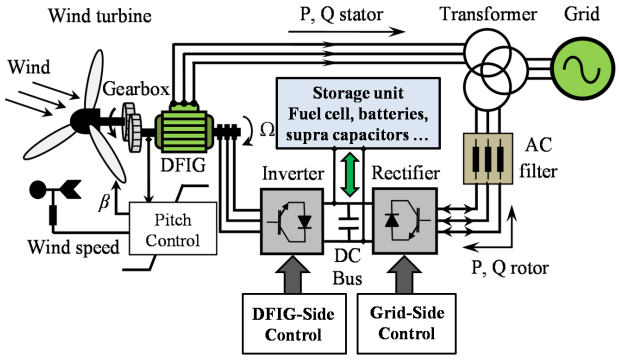

Fig. 1. WECS based a DFIG configuration including a storage unit.

This arrangement provides flexibility of operation in subsynchronous and supersynchronous speeds in both generating and motoring modes (±30% around the synchronous speed). The power inverter needs to handle a fraction (25-30%) of the total power to achieve full control of the generator.

This study analyses by numerical simulations the wind energy conversion of 1.5 MW wind turbine allowing the production of a constant power to the grid and including a storage unit. The incorporation of a battery or other energy storage device in the DC-link enables temporary storage of energy and therefore, the ability to provide constant output active power, which is both deterministic and resistant to wind speed fluctuations [3]. More, good power quality of generators is critical and for this reason, independent control of active and reactive powers is vital [4]. To do this, direct power control (DPC) technique of the double fed induction generator is studied.

The DPC strategy was developed and presented in 1998 by T. Noguchi [5-6] and applied to DFIG in 2006 by L. Xu [7]. DPC is characterized by its fast dynamic response, simple structure and robust response against parameter variations and it does not utilize a rotor current control loops. In the proposed DPC strategy, the active and reactive powers are

estimated, using current measurements, and controlled directly with hysteresis controllers and a switching table similar to the one used in direct torque control (DTC) applied for AC machines [7-8]. Relevant simulation results are presented and discussed to validate the performance of the proposed method of control and show the interest of the energy storage unit in such wind energy conversion systems.

2. Modeling of the DFIG

In the synchronous *d-q* reference frame rotating at ω_s speed, the model of the DFIG is given by the following equations:

Stator voltage components:

$$\begin{cases} V_{ds} = R_s I_{ds} + \dfrac{d}{dt}\psi_{ds} - \omega_s \psi_{qs} \\ V_{qs} = R_s I_{qs} + \dfrac{d}{dt}\psi_{qs} + \omega_s \psi_{ds} \end{cases} \quad (1)$$

Rotor components:

$$\begin{cases} V_{dr} = R_r I_{dr} + \dfrac{d}{dt}\psi_{dr} - (\omega_s - \omega_r)\psi_{qr} \\ V_{qr} = R_r I_{qr} + \dfrac{d}{dt}\psi_{qr} + (\omega_s - \omega_r)\psi_{dr} \end{cases} \quad (2)$$

Stator flux components:

$$\begin{cases} \psi_{ds} = L_s I_{ds} + L_m I_{dr} \\ \psi_{qs} = L_s I_{qs} + L_m I_{qr} \end{cases} \quad (3)$$

Rotor flux components:

$$\begin{cases} \psi_{dr} = L_r I_{dr} + L_m I_{ds} \\ \psi_{qr} = L_r I_{qr} + L_m I_{qs} \end{cases} \quad (4)$$

DFIG electromagnetic torque:

$$T_{em} = -\frac{3}{2} p \frac{L_m}{L_r}\left(\psi_{ds} I_{qr} - \psi_{qs} I_{dr}\right) \quad (5)$$

Let us note that this torque represents a disturbance for the wind turbine and takes a negative value.

Mechanical equation:

$$T_t = T_{em} + J\frac{d\Omega_r}{dt} + f_r \Omega_r \quad (6)$$

Generator active and reactive powers at the stator side are given by the expressions:

$$\begin{cases} P_s = \dfrac{3}{2}\left(V_{ds} I_{ds} + V_{qs} I_{qs}\right) \\ Q_s = \dfrac{3}{2}\left(V_{qs} I_{ds} - V_{ds} I_{qs}\right) \end{cases} \quad (7)$$

3. The simplified model of DFIG

The rotor-side converter is controlled in a synchronously rotating *d-q* axis frame, with the d-axis oriented along the stator flux vector position (Fig. 2). In this approach, decoupled control between the stator active and reactive powers is obtained. The influence of the stator resistance can be neglected and the stator flux can be held constant as the stator is connected to the grid. Consequently [9]:

$$\psi_{ds} = \psi_s \quad and \quad \psi_{qs} = 0 \quad (8)$$

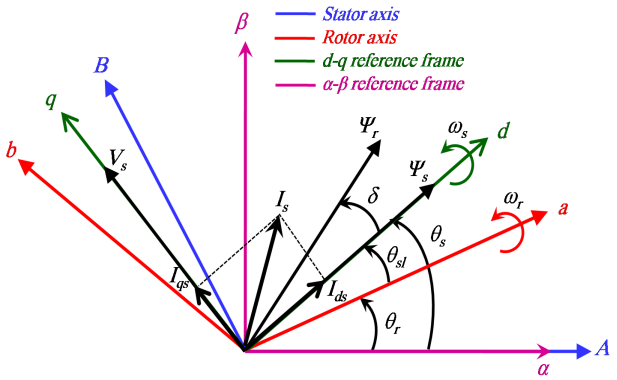

Fig. 2. Stator field oriented control technique.

$$\begin{cases} V_{ds} = 0 \\ V_{qs} = V_s = \omega_s . \psi_s \end{cases} \quad (9)$$

$$\begin{cases} \psi_s = L_s I_{ds} + L_m I_{dr} \\ 0 = L_s I_{qs} + L_m I_{qr} \end{cases} \quad (10)$$

$$\begin{cases} I_{ds} = \dfrac{\psi_s}{L_s} - \dfrac{L_m}{L_r} I_{dr} \\ I_{qs} = -\dfrac{L_m}{L_s} I_{qr} \end{cases} \quad (11)$$

$$\begin{cases} P_s = \dfrac{3}{2} V_s I_{qs} \\ Q_s = \dfrac{3}{2} V_s I_{ds} \end{cases} \quad (12)$$

Replacing the stator currents by their expressions given in (11), the equations below are expressed:

$$\begin{cases} P_s = -\dfrac{3}{2}\dfrac{L_m}{L_s} V_s I_{qr} \\ Q_s = \dfrac{3}{2} V_s \left(\dfrac{V_s}{L_s . \omega_s} - \dfrac{L_m}{L_s} I_{dr}\right) \end{cases} \quad (13)$$

The electromagnetic torque is as follows:

$$T_{em} = -\frac{3}{2} p \frac{L_m}{L_s} \psi_s I_{qr} \quad (14)$$

Rotor voltages can be expressed by:

$$\begin{cases} V_{dr} = R_r I_{dr} - g\omega_s \left(L_r - \dfrac{L_m^{\,2}}{L_s} \right) I_{qr} \\ V_{qr} = R_r I_{qr} + g\omega_s \left(L_r - \dfrac{L_m^{\,2}}{L_s} \right) I_{dr} + g \dfrac{L_m V_s}{L_s} \end{cases} \quad (15)$$

The resulting bloc diagram of the DFIG is presented in Fig. 3.

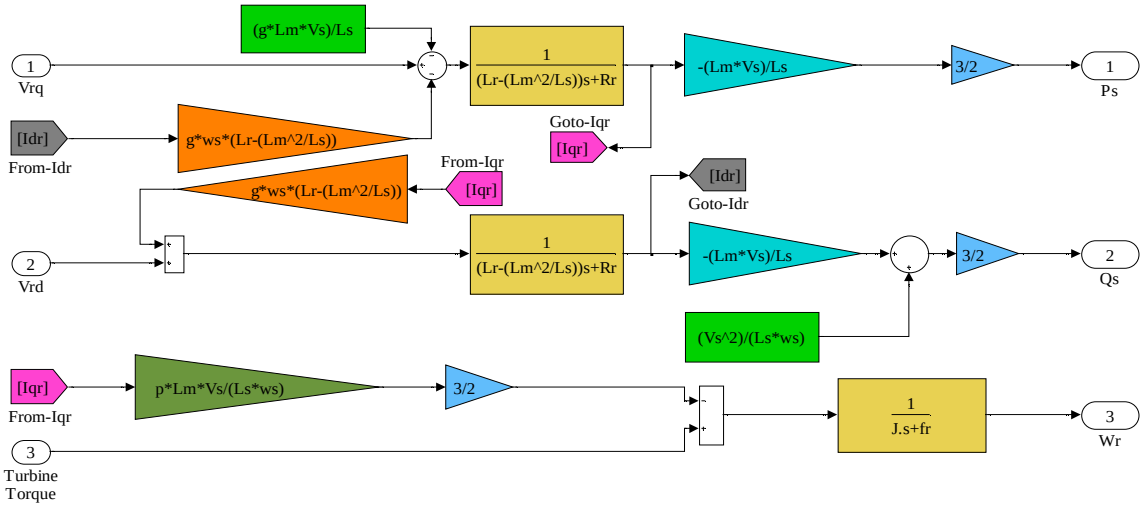

Fig.3. The bloc digram of the simplified DFIG in Simulink.

4. Direct power control strategy

The DPC is based on the same control principles as the DTC technique, the unique difference is the directly controlled variables. In the case of the DTC, the electromagnetic torque and the rotor flux are directly controlled while in the DPC, the stator active and reactive powers are controlled. First a conceptual study of the conventional DPC technique will be carried out. In this case, we present the DPC by using tow levels voltage source inverter (2L-VSI) which supplies the rotor windings as we shown in Fig. 4.

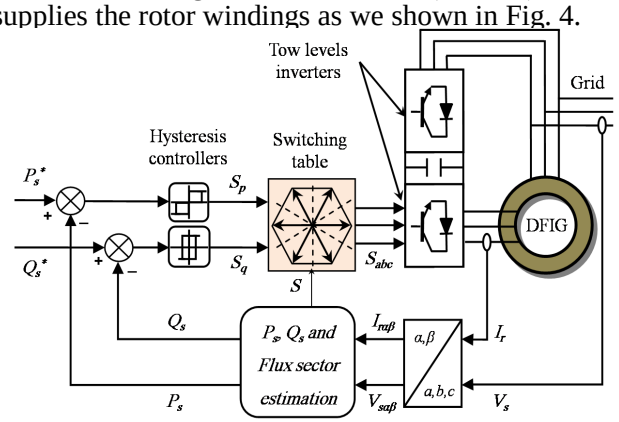

Fig. 4. Schematic diagram of DPC strategy for DFIG.

4.1 Stator active and reactive power estimation

Instead of measuring the tow powers on the line, we capture the rotor currents, and estimate P_s and Q_s. This approach gives an anticipated control of the powers in the stator windings. By using the stator flux oriented control and pervious equations presented in section III, we can find the relations of P_s and Q_s according to both components of the rotor flux in the stationary α_r-β_r reference frame, and we can get:

$$\begin{cases} P_s = -\dfrac{3}{2} \dfrac{L_m}{\sigma L_s L_r} V_s \psi_{\beta r} \\ Q_s = \dfrac{3}{2} V_s \left(\dfrac{1}{\sigma L_s} \psi_s - \dfrac{L_m}{\sigma L_s L_r} \psi_{\alpha r} \right) \end{cases} \quad (16)$$

Where:

$$\begin{cases} \psi_{\alpha r} = \left(L_r - \dfrac{L_m^{\,2}}{L_s} \right) I_{\alpha r} + \dfrac{L_m}{L_s} \psi_s \\ \psi_{\beta r} = \left(L_r - \dfrac{L_m^{\,2}}{L_s} \right) I_{\beta r} \\ \left| \overline{\psi}_s \right| = \dfrac{\left| \overline{V}_s \right|}{\omega_s} \end{cases} \quad (17)$$

If we introducing the flux power angle δ between stator and rotor flux space vectors, P_s and Q_s become:

$$\begin{cases} P_s = -\dfrac{3}{2} \dfrac{L_m}{\sigma L_s L_r} \omega_s \left| \psi_s \right| \left| \psi_r \right| \sin\delta \\ Q_s = \dfrac{3}{2} \dfrac{\omega_s}{\sigma L_s} \left| \psi_s \right| \left(\dfrac{L_m}{L_r} \left| \psi_r \right| \cos\delta - \left| \psi_s \right| \right) \end{cases} \quad (18)$$

Differentiating (18) results in the following equations:

$$\begin{cases} \dfrac{dP_s}{dt} = -\dfrac{3}{2}\dfrac{L_m\omega_s}{\sigma L_s L_r}|\psi_s|\dfrac{d(|\psi_r|\sin\delta)}{dt} \\ \dfrac{dQ_s}{dt} = \dfrac{3}{2}\dfrac{L_m\omega_s}{\sigma L_s L_r}|\psi_s|\dfrac{d(|\psi_r|\cos\delta)}{dt} \end{cases} \quad (19)$$

As we see in (19), these last two expressions show that the stator active and reactive powers can be controlled by modifying the relative angle between the rotor and stator flux space vectors and their amplitudes. This effect is illustrated in the next sections.

4.2 Hysteresis comparators and switching table

The calculated active and reactive powers are compared with their reference values in their corresponding hysteresis comparators as are shown in Fig. 5-a and Fig. 5-b, with S_p and S_q are the outputs signal of active and reactive power controllers respectively.

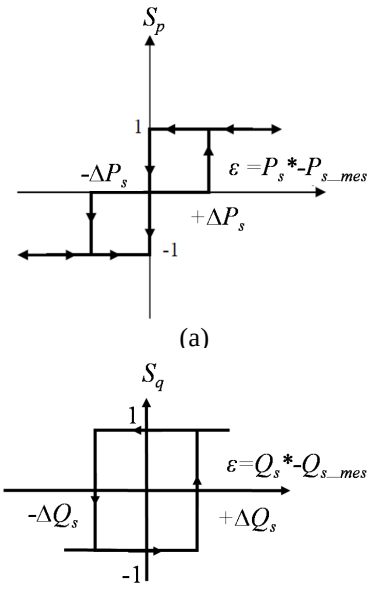

Fig. 5. Hysteresis powers controllers: (a) for active power and (b) for reactive power.

The outputs of the comparators with the number of sector at which the rotor flux space vector is located are fed to a switching table to select an appropriate inverter voltage vector. The selected voltage vector will be applied to the DFIG at the end of the sample time. [5]

Eight switching combinations can be selected in a voltage source inverter, two of which determine zero voltage vectors and the others generate six equally spaced voltage vectors having the same amplitude. According to the principle of operation of DPC, the selection of a voltage vector is made to maintain the active and reactive powers within the limits of two hysteresis bands.

For this purpose, the evolution space of ψ_r in the considered reference frame is divided into six sectors; this choice is dictated by preoccupation with a more rigorous control, and such as:

$$-\frac{\pi}{6} + (k-1)\frac{\pi}{3} \le \delta(k) \le \frac{\pi}{6} + (k-1)\frac{\pi}{3} \quad (20)$$

With: $k=1, 2\ldots6$

The digitized error signal S_p and S_q and the rotor flux sector are input to the switching table in which every switching state S_a, S_b and S_c of the converter is stored as shown in Table 1.

Table 1
Switching table with zero voltage vectors

S_q	1			-1		
S_p	1	0	-1	1	0	-1
Sector 1	V_5	V_7	V_3	V_6	V_0	V_2
Sector 2	V_6	V_0	V_4	V_1	V_7	V_3
Sector 3	V_1	V_7	V_5	V_2	V_0	V_4
Sector 4	V_2	V_0	V_6	V_3	V_7	V_5
Sector 5	V_3	V_7	V_1	V_4	V_0	V_6
Sector 6	V_4	V_0	V_2	V_5	V_7	V_1

4.3 Rotor active voltage vectors effect on powers

Considering that the stator flux space vector amplitude is constant, the stator active and reactive powers only depend on the relative angle between the fluxes *(δ)*, and the rotor flux space vector amplitude. Considering anti-clockwise direction of rotation of the flux vectors in the rotor reference frame to be positive, it may be noted that ψ_s is ahead ψ_r in motoring mode of operation (Fig. 6-a) and ψ_s is behind ψ_r in generating mode (Fig. 6-b). In the rotor reference frame the flux vectors rotate in the positive direction at subsynchronous speeds, remain stationary at synchronous speed and start rotating in the negative direction at supersynchronous speeds. [8]

Assuming that the rotor flux is located in the first sector, the application of voltages vectors V_2 and V_3 results in a decrease in the stator active power whereas, the application of vectors V_5 and V_6 would increase it. In the other hand, the application of V_2 and V_6 would decrease the reactive power drawn from the stator side, while V_3 and V_5 would increase it.

As a generalization it can therefore, be said that if the rotor flux resides in the k^{th} sector, where k = 1, 2, …6, the application of voltage vectors V_{k+1} and V_{k+2} would decrease the delivered stator active power, while the vectors V_{k-1} and V_{k-2} would increase it. Moreover, the application of V_{k+1} and V_{k-1} would decrease (-) the delivered reactive power, while V_{k+2} and V_{k-2} would increase it (+), while the zero voltage vectors have a negligeted (0) effect in Q_s. We note

that the reactive power control is the same in motor and generator operation modes. [8]

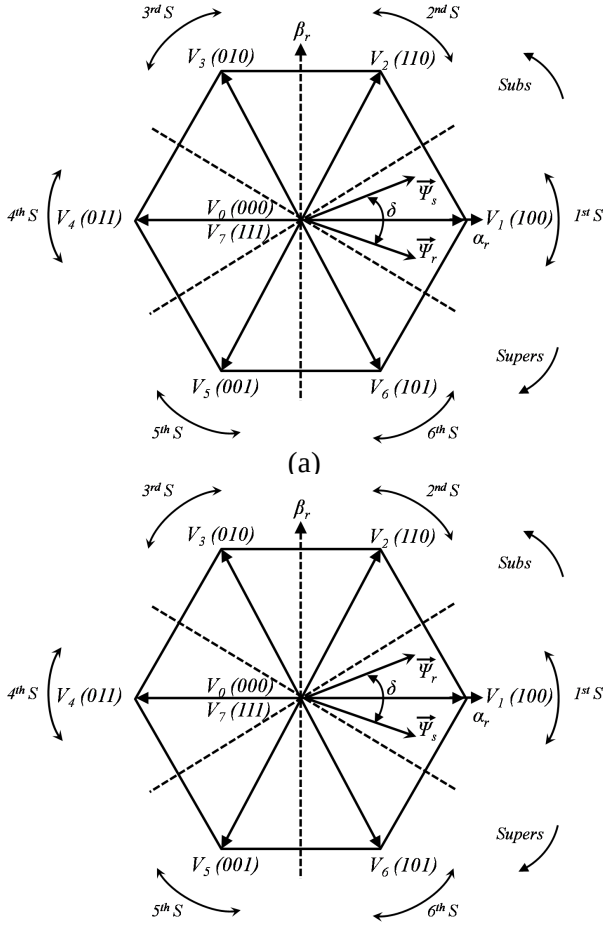

Fig. 6. Flux vectors in rotor coordinates: (a) for motoring mode and (b) for generating mode.

The expected direction of change in Q_s due to the application of any switching state in the different sectors can be summarized in Table 2.

Table 2
Expected direction of change in Q_s

	V_0	V_1	V_2	V_3	V_4	V_5	V_6	V_7
Sector 1	0	0	-	+	0	+	-	0
Sector 2	0	-	0	-	+	0	+	0
Sector 3	0	+	-	0	-	+	0	0
Sector 4	0	0	+	-	0	-	+	0
Sector 5	0	+	0	+	-	0	-	0
Sector 6	0	-	+	0	+	-	0	0

In case of discrepancy, the current sector must be updated according to Table 3 [10], by shifting its position clockwise (-1), anti-clockwise (+1), or just keeping its previous position (0). The DPC sampling period must be small enough so as to never miss the shift of the rotor flux between two adjacent sectors. It may however, be noted that in a particular sector not all vectors will be applied. For example, in the k^{th} sector, vectors V_k and V_{k+3} will never be applied (Table 3).

Table 3
Sector update table

	V_0	V_1	V_2	V_3	V_4	V_5	V_6	V_7
Sector 1	0	0	-1	+1	0	-1	+1	0
Sector 2	0	+1	0	-1	+1	0	-1	0
Sector 3	0	-1	+1	0	-1	+1	0	0
Sector 4	0	0	-1	+1	0	-1	+1	0
Sector 5	0	+1	0	-1	+1	0	-1	0
Sector 6	0	-1	+1	0	-1	+1	0	0

4.4 Zero voltage vector effect on powers

We notice that the order of voltage vectors is opposite in subsynchronous operation with respect to supersynchronous operation (Fig. 7). The zero voltage vectors V_0 and V_7 stall the rotor flux vector without affecting its magnitude. Their effect on active power is thus opposite in subsynchronous and supersynchronous operation.

Since a zero vector does not change the magnitude of the rotor flux its effect on the reactive power is rather small. Nevertheless, there is some small change in Q_s; its effect being dependent on whether the angle between the stator and rotor fluxes increases or decreases due to the application of a zero vector. An increase (↑) in angular separation between the two fluxes reduces (↓) ψ_{sr} resulting in an increment (↑) of Q_s drawn from the stator side. The converse is true when δ reduces. It is observed that the change in Q_s due to the application of the zero vectors is different in all the 4 modes of operation. This is summarized in Table 4.

Table 4
Zero voltage vector effects on reactive power

Speed	Motoring	Generating
Subs	$\delta\uparrow \Rightarrow \psi_{sr}\downarrow \Rightarrow Q_s\uparrow$	$\delta\downarrow \Rightarrow \psi_{sr}\uparrow \Rightarrow Q_s\downarrow$
Supers	$\delta\downarrow \Rightarrow \psi_{sr}\uparrow \Rightarrow Q_s\downarrow$	$\delta\uparrow \Rightarrow \psi_{sr}\downarrow \Rightarrow Q_s\uparrow$

5. Storage unit

A long duration storage unit is included in the wind energy conversion system. Battery, super-capacitor or fuel cell could be used to restore electrical power when the wind conditions do not allow constant power generation by the DFIG. Other storage systems, like flywheel [11-12], are not well suited because a large amount of energy for a long duration is needed in our system.

The long duration storage unit connected to the DC bus allows producing a constant active power to the grid for all wind conditions. In high wind speed conditions, the DFIG provides energy to the network and refills the storage unit whereas in insufficient wind conditions, the storage unit allows compensating the lack of energy. This is a very useful operation for wind turbine grid connection.

The pitch control achieves the maximum efficiency of the turbine. It is also possible to turn off the turbine when wind speed is too large to prevent any mechanical damage. For a given wind speed, the power reference is calculated and subtracted from the constant power injected to the grid to fix the power reference for the storage unit. This power can be positive or negative according to wind speed conditions.

The power can be positive or negative if the generator performs at hyper or hypo synchronous conditions and when the storage unit absorbs power from the wind turbine or provides power to the grid. The storage unit is controlled in power for charge and discharge, and the power stored in the battery is calculated by:

$$P_{stored} = P_s - 0.75MW \quad (21)$$

And the power injected to the grid is given by the expression:

$$P_{grid} = P_s^* - P_{stored} \quad (22)$$

Where P_s and P_s^* are the produced and reference active power respectively.

6. Simulation results

In this section, we present simulation results for a 1.5 MW DFIG associated with a 0.75 MW storage unit. The wind turbine is also supposed to inject a constant power of 0.75 MW into the grid for all wind conditions. The direct power control strategy is simulated at 100 µs sampling period. Simulation results for DPC are presented in Fig. 7.

Simulations are performed with a random wind speed, varying between 2 and 20 m/s (Fig. 7-a).

The active power of the DFIG follows the power reference calculated from the wind speed. This power is limited by the generator nominal power (1.5 MW). Simulation results for active power of the DFIG demonstrate the impossibility of generating a constant active power equal to 0.75 MW under all wind speed conditions (Fig. 7-b).

Simulation results for power of the storage unit correspond to a positive power when charging the storage unit and a negative power when feeding the grid (Fig. 7-c). This power allows compensating active power of the DFIG when wind conditions do not allow generating 0.75 MW.

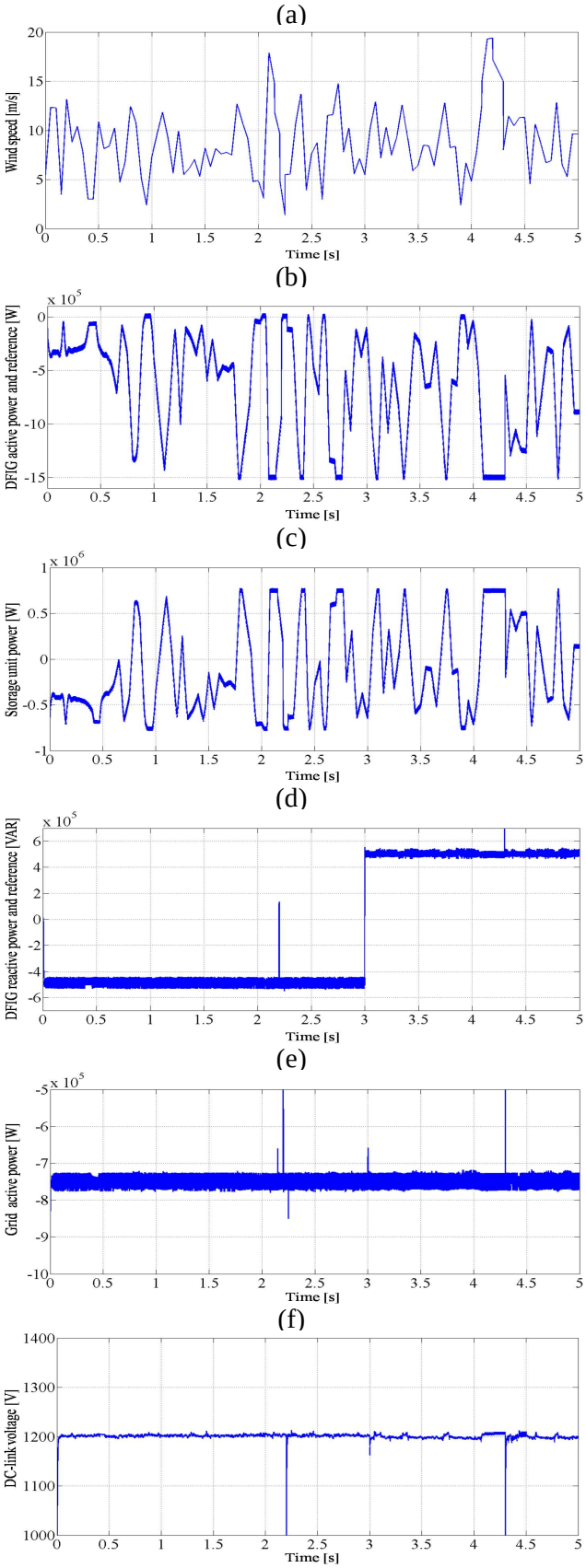

Fig. 7. Direct power control strategy responses.

A step is applied on the reactive power reference (Fig. 7-b), from -0.5 MVAR to +0.5 MVAR, at t = 3s, (The negative sign "-" refers to the generation of active power and to the absorption of reactive power). The reactive power is correctly regulated and the effect of the simulated step at t = 3s is negligible (Fig. 7.d).

On the Fig. 7-e, the produced power is kept constant (0.75 MW) for all wind conditions. This corresponds to the sum of the DFIG and storage unit powers. Consequently, this wind energy conversion system can be assimilated as a constant generator for active power.

A slight modification to the DC-link voltage shown in Fig. 7-f, it's made by including battery storage.

7. Conclusion

The DFIG is nowadays a popular choice for wind energy conversion systems. This popularity is mostly due to its ability for large variable speed drive. In this paper the direct power control strategy has been presented; this technique has been used for reference tracking and decoupling of active and reactive powers exchanged between the stator of the DFIG and the grid by controlling the rotor converter. DFIG is often used in wind energy conversion system, that's why the model of the DFIG has been associated with a wind turbine model controlled with MPPT strategy. The whole system thus constituted permits to control the DFIG at subsynchronous and supersynchronous speeds.

The incorporation of a battery or other energy storage device in the DC-link enables temporary storage of energy and therefore, the ability to provide constant active power injected to the grid, which is both deterministic and resistant to wind speed fluctuations. Simulation results demonstrate the effectiveness of the DPC strategy to control active and reactive power independently with good performances. On the other hand, they prove the large interest of energy storage in such wind energy conversion systems.

Appendix

Table 5
Wind turbine parameters

Blade radius, R	35.25 m
Number of blades	3
Gearbox ratio, G	90
Moment of inertia, J	1000 Kg.m^2
Viscous friction coefficient, f_r	0.0024 N.m.s^{-1}
Cut-in wind speed	4 m/s
Cut-out wind speed	25 m/s
Nominal wind speed, v	16 m/s

Table 6
Doubly fed induction generator parameters

Rated power, P_n	1.5 MW
Stator rated voltage, V_s	398/690 V
Rated current, I_n	1900 A
Rated DC-Link voltage U_{DC}	1200 V
Stator rated frequency, f	50 Hz
Stator inductance, L_s	0.0137 H
Rotor inductance, L_r	0.0136 H
Mutual inductance, L_m	0.0135 H
Stator resistance, R_s	0.012 Ω
Rotor resistance, R_r	0.021 Ω
Number of pair of poles, p	2

References

1. Petersson, A.: *Analysis, modeling and control of doubly fed induction generators for wind turbines.* PhD thesis, Champers University of Technology, Sweden, 2005.

2. EL Aimani S., François B., Minne F., and Robyns B.: *Modelling and simulation of doubly fed induction generators for variable speed wind turbines integrated in a distribution network.* In: 10th European conference on power electronics and applications, Toulouse, France, September 2–4, 2003.

3. Boyette A., Poure P., Saadate S.: *Direct and indirect control of a Doubly Fed Induction Generator wind turbine including a storage unit.* In: 32th edition of Industrial Electronics Conference IECON'2006, IEEE, Paris, France, November 6-10, 2006, p. 2517–2522.

4. Hennessy T., Kuntz M.: *The multiple benefits of integrating electricity storage with wind energy*. In: Power Engineering Society General Meeting, 2005. IEEE, June 12-16, 2005, p. 1388–1390.

5. Takahashi, I., Noguchi, T.: *A new quick-response and high-efficiency control strategy of an induction motor*. In: IEEE Trans. Ind. Appl., IA-22 (1986), No.5, October 1986, p. 820-827.

6. Noguchi, T., Tomiki, H., Kondo, S., Takahashi, I.: *Direct power control of PWM converter without power-source voltage sensors.* In: IEEE Trans. Ind. Applications, 34 (1998), May/June 1998, p. 473-479.

7. Xu, L., Cartwright, P.: *Direct active and reactive power control of DFIG for wind energy generation"*, IEEE Trans. Energy Conversion, 21 (2006), No.3, September 2006, p. 750-758.

8. Datta, R., Ranganathan, V.T.: *Direct power control of grid-connected wound rotor induction machine without rotor position sensors.* In: IEEE Trans. Power Electron., 16 (2001), No.3, May 2001, p. 390-399.

9. Hopfensperger, B., Atkinson, D.J., Lakin, R.: *Stator-flux-oriented control of a doubly-fed induction machine*

with and without position encoder. In: IEE Proc.-Electr. Power Applications, 147 (2000), No.4, July 2000, p. 241-250.

10. Tremblay, E., Atayde, S., Chandra, A.: *Comparative study of control strategies for the doubly fed induction generator in wind energy conversion systems: A DSP-based implementation approach.* In: IEEE Trans. Sustainable Energy, 2 (2011), No.3, July 2011, p. 288-299.

11. Ghedamsi, K., Aouzellag, D., Berkouk, E.M.: *Control of wind generator associated to a flywheel energy storage system.* In: Renewable energy, Elsevier, 33 (2008), No.9, 2008, p. 2145-2156.

12. Hakagi, H., Sato, H.: *Control and Performance of a Doubly-Fed Induction Machine Intended for a Flywheel Energy Storage System.* In: IEEE Transactions on Power Electronics, 17 (2002), No.1, January 2002, p. 109-116.